

Solitary Waves and Interacting Longons in Galerkin-truncated Systems

Jian-Zhou Zhu (朱建州)^{1,*}

¹Su-Cheng Centre for Fundamental and Interdisciplinary
Sciences, Gaochun, Nanjing 211316, China

Abstract

The compacton, peakon, and Burgers-Hopf equations regularized by the Galerkin truncation preserving finite Fourier modes are found to support new travelling waves and interacting solitonic structures amidst weaker less-ordered components ('longons'). Different perspectives focusing on the zero-Hamiltonian solitonic, chaotic-looking, and stationary longons are also offered.

The compactons and/or peakons [1–4] are rough and can be regularized by the Galerkin truncation preserving finite Fourier modes, resembling yet differing from the Korteweg-de Vries (KdV) regularization of the Burgers-Hopf (BH) equation. Such or similar truncations are well-known in analysis, computation, and (effective field) theories.

Let $v(x, t)$ solve, with x -period 2π and $v_0 = v(x, 0)$,

$$v_t + vv_x = a. \tag{1}$$

$a = 0$, $\mp v_{txx}/9 \mp 2v_x v_{xx}/27 \mp v v_{xxx}/27$, μv_{xxx} , and $v(v^2)_{xxx}$ identify, respectively, the BH, compacton/peakon (CP [1, 2]), KdV and Rosenau-Hyman [4] compacton [RH or $K(2, 2)$] equations. In the CP model [reverting to the convenient form $v_t \pm v_{txx} + 3vv_x = \mp 2v_x v_{xx} \mp v v_{xxx}$ with the x -rescaling factor 3 from now on], the upper signs correspond to the compacton and the lower signs to the Camassa-Holm (CH) peakon model [3].

We work in the period $[0, 2\pi)$ and then have $\hat{v}_k = \int_0^{2\pi} \frac{v}{2\pi} e^{-ikx} dx$, with complex conjugacy (*c.c.*) $\hat{v}_k^* = \hat{v}_{-k}$ for reality. Additionally, $v\partial_x v = \sum_k \hat{b}_k e^{ikx}$ where $\hat{b}_k = \frac{ik}{2} \sum_p \hat{v}_p \hat{v}_{k-p}$ and $\hat{t}^2 = -1$. For v_0 well-prepared in ${}^K\mathbb{G} = \{k : -K \leq k \leq K\}$ ("Galerkin space" hereafter), we can calculate each \hat{b}_m for $K < |m| (\leq 2K)$. In the BH case, setting \hat{a}_m to be ${}^K\hat{g}_m = \hat{b}_m$ for $m \notin {}^K\mathbb{G}$ and 0 otherwise results in Galerkin truncation: for all $m \notin {}^K\mathbb{G}$, $\hat{v}_m(t) \equiv 0$ ($t > 0$), thus the Galerkin-regularized BH (GrBH), and, similarly, the GrKdV, GrCP, or, GrCH and GrRH systems.

Define $P_K v(x) := \sum_{|k| \leq K} \hat{v}_k \exp\{\hat{t}kx\} =: u$, $B := u^2/2$ and ${}^K G := B - P_K B$. Then follows the GrBH equation [5]

$$Du/Dt := \partial_t u + \partial_x B = \partial_x {}^K G; \quad u_0 = P_K v_0. \tag{2}$$

The Galerkin force ${}^K g = \partial_x {}^K G$, with ${}^K \hat{g}_m$ for $K < |m| \leq 2K$, is excited when there exists $\hat{u}_k \neq 0$ with $k > K/2$.

The CP Hamiltonian operator $J_{CP} = -2\pi(\partial_x \pm \partial_x^3)$ in Fourier representation still applies with truncation and is inherited by GrCP, just like $J_{KdV} = -2\pi\partial_x$ by GrKdV [6]. The GrBH

reduction replaces the reduced Hamiltonian $\mathcal{H}_{BH} = \int_0^{2\pi} \frac{u^3 dx}{12\pi}$ with [7]

$$\mathcal{H} = \sum_{p,q,k=p+q \in K\mathbb{G}} \hat{u}_k^* \hat{u}_p \hat{u}_q / 6, \quad (3)$$

thus the Galerkin interaction potential ${}^K\mathcal{G} = \mathcal{H}_{BH} - \mathcal{H}$. The other reduced Hamiltonian operator $J'_{BH} := -(u\partial_x + \partial_x u)/3$ involves u and is not transferable to GrBH to facilitate the bi- or tri-Hamiltonian machinery with integrability in that sense [1]. Actually, only three GrBH invariants, \mathcal{H} , $\mathcal{E} = \int_0^{2\pi} \frac{P_K B dx}{4\pi}$ and $\mathcal{M} = \hat{u}_0 = \int_0^{2\pi} \frac{u dx}{2\pi}$ are known for general K ; similarly for the GrKdV and GrCP situations, with, e.g., $\mathcal{H}_{CP} = \int_0^{2\pi} \frac{v^3 \mp v(\partial_x v)^2}{4\pi} dx$ and, accordingly, \mathcal{M}_{CP} and \mathcal{E}_{CP} , and, their truncated versions. By Galilean invariance, \mathcal{M} is taken to be zero or truncated in this study, and K is effectively the number of available modes with $2K$ degrees of freedom.

Effective field theories in particle and condensed matter physics often entail truncations, such as those involving momentum, akin to wavenumber restrictions. Should the truncation prove ill-suited or if physical limitations intrude, our findings on classical systems suggest the potential emergence of novel particles — be they fictitious or genuine.

Solitary waves and interacting longons.— The Gr-system solutions of the form $u^\#(x, t) = u^\#(\zeta)$ with $\zeta = x - \lambda t$ exist:

In Fourier space, GrBH traveling waves satisfy

$$\partial_i \hat{u}_k^\# = -\frac{\hat{i}k}{2} \sum_{p,q,p+q=k \in K\mathbb{G}} \hat{u}_p^\# \hat{u}_q^\# = -\hat{i}\lambda k \hat{u}_k^\#. \quad (4)$$

For $\lambda = 0$, immediate examples include that with a single mode in $(K/2, K]$; while, with an arbitrary phase parameter x_0 , $u^\# \propto 2 \cos[K(x - x_0)/3] - \cos[K(x - x_0)]$ for $\text{mod}(K, 3) = 0$ are less-trivial ones more of which we later will come back to: note, however, with $x_0 = 0$ henceforth, for instance, $u^\# \propto 2 \cos(2x) - \cos(6x)$ can travel freely in ${}^7\mathbb{G}$ without excitations of $|k| = 7$, so another parameter S is naturally introduced below. For moving waves ($\lambda \neq 0$) of L active modes, with $\text{mod}(S, L) = 0$ and $S \leq K < (L + 1)S/L$, we find, by straightforward calculation with $L = 2$,

$$u^\# = 2\sqrt{2}|\lambda| \cos(S\zeta/2) + 2\lambda \cos(S\zeta). \quad (5)$$

And, taking $\lambda > 0$, with $\theta = S\zeta$, we have a three-mode wave,

$$u^\# = \lambda[-2\chi_1 \cos(\theta/3) + \chi_2 \cos(2\theta/3) - \chi_1\chi_2 \cos \theta] \quad (6)$$

where $\chi_1 = \sqrt{\frac{5-\sqrt{5}}{5}}$ and $\chi_2 = \sqrt{5} - 1$. Accordingly, $Kg^\# \propto S\lambda^2$; for example, corresponding to Eq. (5),

$$Kg^\# = -(S\lambda^2)[3\sqrt{2}\sin(3\theta/2) + 4\sin(2\theta)]/2. \quad (7)$$

Similarly, Eq. (5) extends to GrKdV-GrRH waves

$$u^\# = 2\sqrt{\frac{\lambda - \mu S^2}{1 + 2\nu S^2}}\chi \cos \frac{\theta}{2} + \chi \cos \theta \quad (8)$$

with $\chi = (4\lambda - \mu S^2)/(2 + \nu S^2)$; and, for the GrCP model,

$$\frac{u^\#}{\lambda} = \frac{4}{3}\sqrt{\frac{2(1 \mp S^2)}{(4 \mp S^2)}}\cos \frac{\theta}{2} + \frac{2}{3}\cos \theta. \quad (9)$$

Many-mode $u^\#$ s can be obtained numerically; e.g., with $\text{mod}(S, 4) = 0$, approximate η s ($\{\eta_1, \eta_2, \eta_3, \eta_4\}$ s) can be found in the ansatz

$$\frac{u^\#}{2\lambda} \approx \eta_1 \cos \frac{\theta}{4} + \eta_2 \cos \frac{\theta}{2} + \eta_3 \cos \frac{3\theta}{4} + \eta_4 \cos \theta. \quad (10)$$

Specifically, $\eta \approx \eta^c = \{-0.507, 0.450, -0.376, 0.292\}$ correspond to a GrBH case resembling the cnoidal wave, except for weaker wiggles between the strong pulses, which is also the case for Eqs. (8) and (9). Wiggle counts grow with mode numbers, as shown in Fig. 1's top and middle panels, using $K = S$ [always so below: other K s ($< S + S/L$) yield the same scenario, modulo quantitative variances.]

Pseudo-spectral computations (discussed later) indicate that the above $u^\#$ s are stable when K equals the number of modes in $u_0^\#$. However, as shown in Fig. 2, for larger K with empty modes in the respective $u_0^\#$, instability eventually transforms the waves into robust states with interacting strong solitonic ‘longons’ (further explained below) amid weaker, less-ordered components (also longons) of various propagating speeds roughly proportional to the signed strengths, featuring more widely separated crests and troughs whose levels vary slightly and periodically over time. The apparently solitonic longons locally resemble the Mexican hat. This is even clearer in larger- K cases, as exemplified later in Fig. 3. There are waves of other shapes, with various organizations of the strong pulses and weak wiggles indicating some symmetry in the solutions (as ‘multiplets’ and ‘supermultiplets’ in particle physics), which were observed in the developing phases but never in the developed solitonic longons (paralleling the absence of quarks and gluons in the free state).

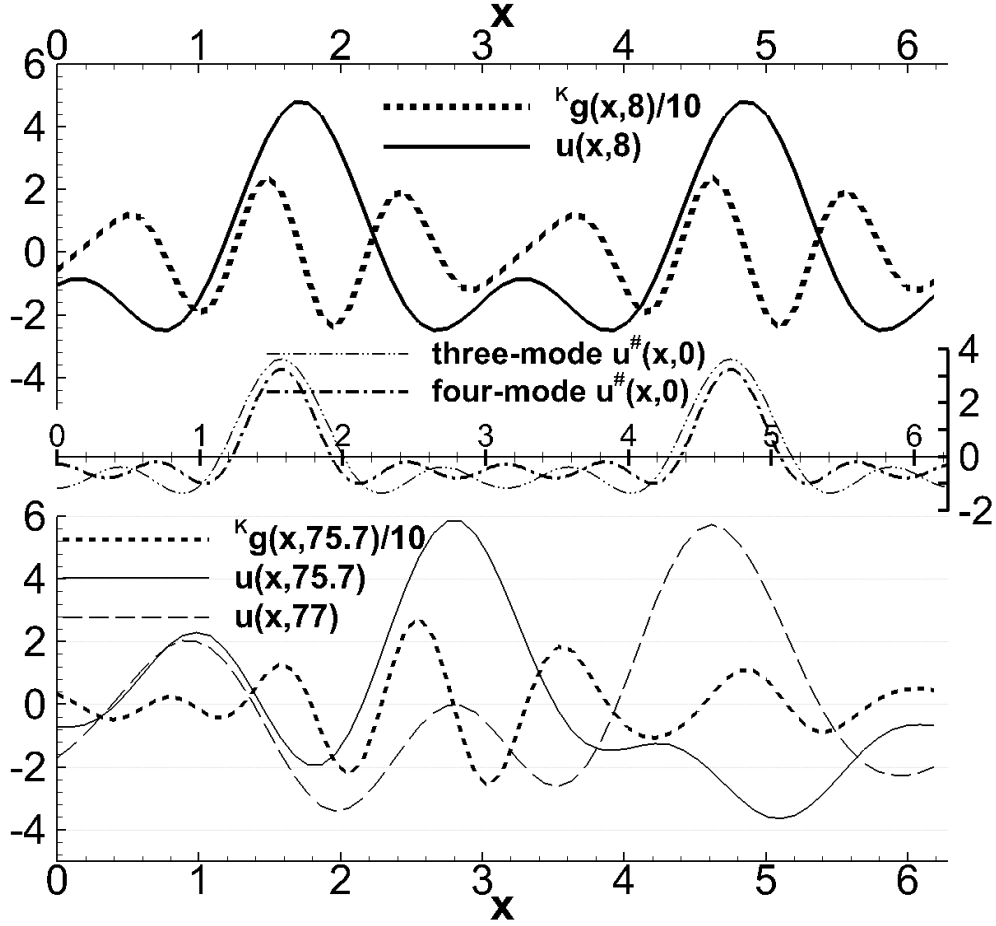


Figure 1. GrBH fields for $K = 4$ and $\lambda = 1$ of the two-mode solitary wave, at two regimes (upper and lower frames): $u(x, t)$ at $t = 8$ obeying Eqs. (5) transitioning to an interacting-longon state at $t = 75.7$ [with $u(x, 77)$ added particularly to show varying crest and trough levels]. The middle frame for the three- and four-mode $u^\#$ s with $\lambda = 1$ at $t = 0$, respectively Eq. (6) for $K = 6$ and Eq. (10) for $K = 8$ with η^c , is inserted to show the similarity and differences. Results of other Gr-systems are of similar fashion and not shown.

After the instability overtakes the solitary waves, the longons exhibit a half-wavelength Kg oscillation within each strong(est) pulse, similar to the $u^\#$ s. This feature is universal across all Gr-systems, with only minor differences in details such as strengths, as partially shown in Fig. 2. The GrCP compacton branch requires rescaling to mitigate the issue of vanishing denominators, yet its outcomes are similar to those of the peakon branch and hence are not presented here. The “universality” is also in the sense that the major features from such a low K ($= 4$) extend to large K s [8], which is further demonstrated by the GrRH

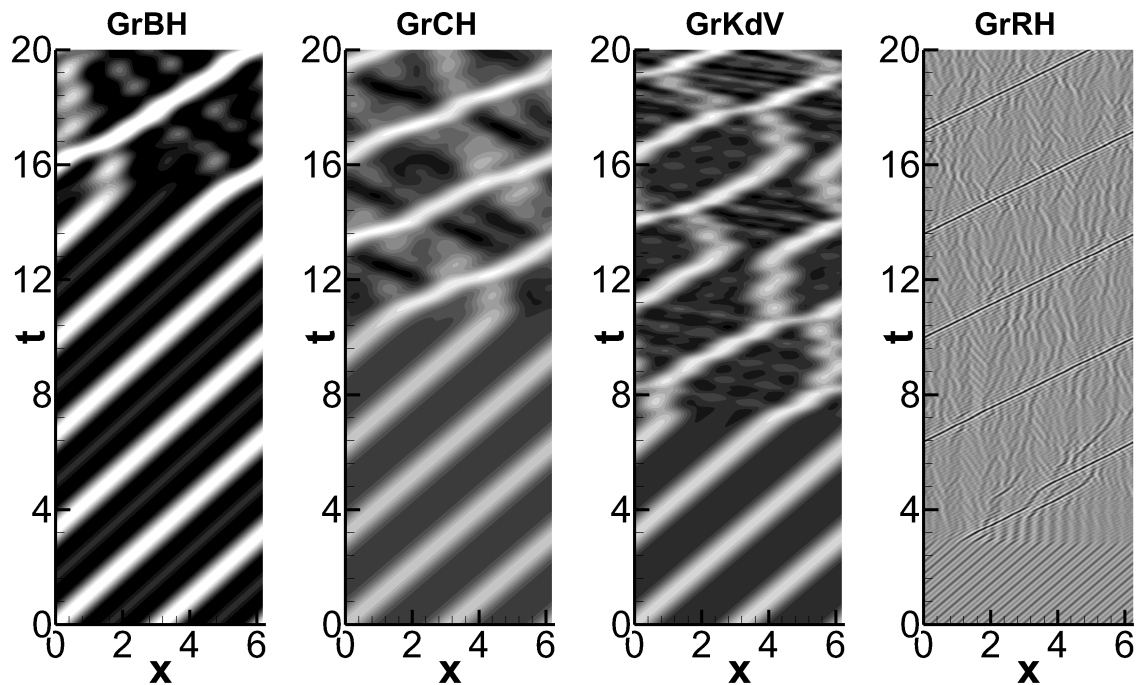


Figure 2. Space-time u -contours of the Gr-systems ($\lambda = 1$): GrBH with $K = 4$, GrCH with $K = 4$ and $\kappa = 0$ (larger u is brighter as can be read from Fig. 1's top frame; similarly for others), GrKdV with $K = 4$ and $\mu = -0.2$, and, GrRH with $K = 32$ and $\nu = -4$.

case with $K = 32$ where a sharp solitonic ‘dark’ (negative-sign) longon emerges subsequent to the solitary wave’s breakdown. The GrKdV case does not have strictly $u^\# \propto \lambda$, so the corresponding results depend, to some extent, on λ a thorough survey of which is however not of interest here.

The high-dimensional Gr-systems, such as the truncated Kadomtsev-Petviashvili and Zakharov-Kuznetsov models, and their nonlinearly dispersive versions [4, 9], similarly admit solitary-wave solutions and, presumably, the longons from the interaction potentials, \mathcal{KG}_S [10]. We will henceforth focus on the minimal GrBH case.

Lattice model point of view.—Let the periodic lattice coordinate satisfy $x_j = x_{j+N}$, whence $v(x_{j+N}) = v(x_j) =: v_j$ for $j = 0, 1, 2, \dots, N-1$, defining a discrete torus \mathbb{T}_N . The theoretical foundation of the (pseudo-)spectral method and the GrBH lattice definition lies in replacing \hat{v}_k defined earlier by the discrete Fourier transform (DFT) for $|k| \leq M$ (with $N-1 = 2M$ here), $\hat{v}_k := \sum_{x_j \in \mathbb{T}_N} \frac{v_j}{N} e^{-ikx_j} = \hat{v}_k + \sum_{i \neq 0} \hat{v}_{k+iN}$. The aliasing error, represented by the second term, can be mitigated using dealiasing techniques like zero-padding or, alternatively speaking,

truncation at $K < N/3$ (“2/3-rule” [11]). Unifying the dealiasing and the Galerkin truncation results in, correspondingly, $\hat{u}_k = \hat{u}_k$ for $u = P_K v$ in the GrBH equation (2), i.e., $\partial_t u_j = -P_K \partial_x u_j^2/2$, so

$$\partial_t u_j = \sum_{\substack{p, q \in \mathbb{K}_G \\ p+q=k \in \mathbb{K}_G}} \sum_{\substack{x_n \in \mathbb{T}_N \\ x_m \in \mathbb{T}_N}} \frac{k u_m u_n e^{\hat{i}(kx_j - px_m - qx_n)}}{2\hat{i}N^2} \quad (11)$$

where the right-hand side in physical-space variables reveals the GrBH lattice dynamics explicitly.

The 2/3-rule ensures sufficient sampling with N sites for the $2K + 1$ mode Gr-continuum, rendering extra sites (e.g., doubling N) dynamically redundant, unlike conventional models. The pseudo-spectral method computes GrBH in Fourier space, evaluating the nonlinear term in physical space via DFT of $P_K u_j^2$, $\partial_t \hat{u}_k = -\frac{\hat{i}k}{2} \sum_{j=0}^{N-1} \frac{P_K(u_j^2)}{N} e^{-\hat{i}kx_j}$. So, the pseudo-spectral computation aligns precisely with the GrBH definition with only errors from the computer roundoff and time discretization.

Since fourth-order Runge-Kutta scheme and its variant (for an approximation below) are used, the numerical results are highly accurate and reliable. Linear analysis (e.g., Lyapunov) of perturbed GrBH solutions indicates generic instability, but identifying physically relevant ones is challenging. And, conventional nonlinear analyses, such as orbital instability analysis, must contend with the unconventional K_g . Here, the numerical results potentially provide clues for further establishing relevant analytical insights.

Hamiltonian effects?—Notably, extremizing \mathcal{H} via

$$\delta(\mathcal{H} - \lambda \mathcal{E})/\delta u = 0 \quad (12)$$

yields Eq. (4). For the large- K GrBH problem, there are in general ${}^K N_k = 2[K + \text{sgn}(|\mathcal{M}|)] - 1 - |k|$ triads satisfying $p + q = k$ for each k . If ${}^K N_k$ were independent of k , then $\hat{u}_k = c(\lambda)$, a real constant uniform over k would extremize \mathcal{H} . Therefore, for large K , with ${}^K N_k$ changing relatively slow with k ,

$$u_0 = [\cos(x) + \cos(2x) + \dots + \cos(Kx)]/\sqrt{K} \quad (13)$$

is an appropriate typical large-Hamiltonian but non-travelling-wave initial data for GrBH.

It turns out that the “universality” of the scenario mentioned earlier further extends, as illustrated in the upper frames of Fig. 3 for $K = 85$ with $\mathcal{H}^2/\mathcal{E}^3 \approx 20.75$: two head-on

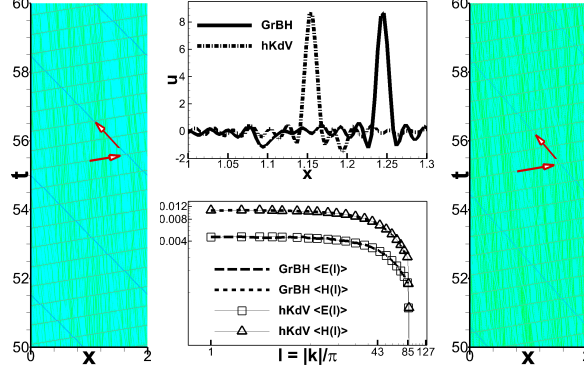


Figure 3. GrBH (left) and hKdV (right) u -contours. The period is normalized from 2π to 2. Snapshots (middle, upper) of the GrBH (at $t = 59.9$) and hKdV (at $t = 59.7$) u -profiles [corresponding to the contours whose color coding can be accordingly read], and, the energy and Hamiltonian spectra (middle, lower). The arrows are added to highlight the propagation of the apparently solitonic longons.

colliding solitonic longons, with their strengths roughly proportional to the respective speeds, travel among the chaotic-looking ones; the latter present “long” pseudo-trajectories, always the case for large- K systems, and may actually also be ‘particles’ as the ‘strange particles’ and ‘resonances’ in particle physics [12]: an important reason for the term “longon”. We may unify the emergence and decay of such ‘particles’ with the notion of chaotization and use terminologies such as ‘thermalization’ alternatively.

Besides the conventional energy spectrum $E(|k|) := \langle |\hat{u}_k|^2 \rangle$, we may define

$$H(|k|) := \sum_p \langle \hat{u}_p \hat{u}_{k-p} \hat{u}_k^* + c.c. \rangle / 6 \quad (14)$$

with $\langle \bullet \rangle$ for time averaging. The energy transfer rate is $T(|k|) := \hat{i} \sum_p \langle \hat{u}_p \hat{u}_{k-p} \hat{u}_k^* - c.c. \rangle / 2$, showing some duality with $H(|k|)$. In GrBH absolute (statistical) equilibrium, $T = 0$ marks the balance of energy transfer, but H provides additional insights into the structures. In the lower frame of Fig. 3(b), E and H are compared to those of a “hyperdispersive”-KdV (hKdV) approximation:

For an appropriate sequence ω_O of the dispersive functions $\omega(n)$ in the model $\hat{a}_n = -\hat{i}\omega(n)\hat{v}_n$ in Eq. (1), with $\omega_O(m) \rightarrow \infty$ for all $m \notin K\mathbb{G}$ and $\omega_O(k) \rightarrow 0$ for all $k \in K\mathbb{G}$, the corresponding hKdV model can be used to approximate the decoupled GrBH sub-dynamics with well-prepared u_0 in $K\mathbb{G}$. The asymptotic GrBH sub-dynamics may be argued directly by the fact

that the intra- and extra-Galerkin frequencies can not match to form a resonant triad with a large jump of $\omega(n)$ in the classical resonant wave theory: the extra-Galerkin modes, if set up initially (“ill-prepared”), however, can have their own dynamics, not of the interest here though. For understanding some physics of dissipation, a choice of a in Eq. (1) in Ref. [13] was the dissipation function $\propto -(k/k_G)^{2O}$ ($K < k_G < K + 1$) for integer $O \rightarrow \infty$, but more consistent with the current situation is hKdV

$$\hat{a}_k = -\hat{i}\omega_O(k)\hat{v}_k; \quad \omega_O = \begin{cases} (\frac{k}{k_G})^{2O+1} & \forall k \notin K\mathbb{G} \\ 0 & \forall k \in K\mathbb{G} \end{cases} \quad (15)$$

For some solitary waves, it is possible to show the convergence to the corresponding explicit expressions of the Gr-systems (such as those discussed earlier) with given K and k_G . In the numerical computations [14] reported in the lower frames of Fig. 3 with correspondingly the same lattice number $N = 512$ and initial data, $k_G = 85.5 = K + 0.5$ and $O = 200$ are used in the hyper-dispersion Model (15), and, to avoid the slow change for $|k|$ near k_G^+ , $\omega_O(k)$ is empirically set to be $750 \operatorname{sgn}(k)(|k| - k_G)$ if $(|k|/k_G)^{401} < 1300$, with the period normalized from 2π to 2. The hKdV structures are close to the GrBH ones in the upper frame of the panel (a). The energy and Hamiltonian spectra, respectively, are also close and show the equipartition tendency at small wavenumbers ($|k| < 10$, say). Solitonic longon pulses approximate the Dirac delta function, thus the asymptotic large-scale energy equipartition; the nonlocal contribution to $H(|k|)$ at small $|k|$ from p is dominated by small- $|p|$ modes, thus also equipartitioned $H(|k|)$. Note $\hat{i}(k/k_G)^{401}\hat{u}_k$ corresponds to a Hamiltonian component $(\partial_x^{200}u)^2/(2k_G^{401})$ which however is minute, due to the smallness of \hat{u}_m for all $m \notin K\mathbb{G}$: the GrBH \mathcal{H} is checked to be well preserved in the approximate model with tiny errors ($< 2\%$).

The spectral and pattern comparisons of similar mixed solitonic and thermalized longon states (longon turbulence [15]) indicate the convergence to GrBH dynamics with the model (15) in the large- O limit (with closer longon turbulence for larger O verified — not shown), which is corroborated by other numerical results with different setups (of various initial data of zero-Hamiltonian or not).

Intuitions, associated to the piecewise-constant $v_0 \sim \sum_k \frac{-2\hat{i}}{(2k+1)\pi} e^{\hat{i}(2k+1)x}$ as a weak solution to the BH equation, suggest a quasi-piecewise-constant (QPC)

$$u_0^{qpcK} = \mathcal{Q} \sum_{|2k+1| \leq K} \frac{-2\hat{i}}{(2k+1)\pi} e^{\hat{i}(2k+1)(x+x_0)}. \quad (16)$$

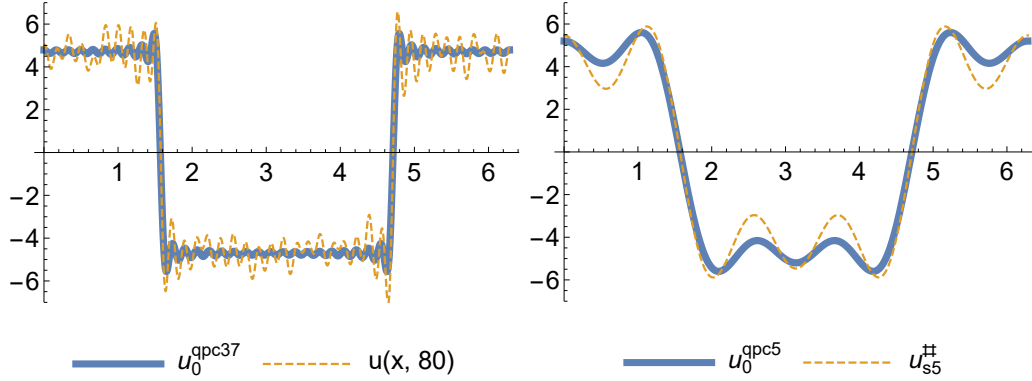


Figure 4. Well-developed $u(x, t)$ at a typical time $t = 80$ from u_0^{qpc37} with $K = 37$ (left), and, $u_{s5}^{\#}$ and u_0^{qpc5} (right); $Q = 3/2$.

Fig. 4 (left panel) shows, among other selectively thermalized or random-like weaker oscillations in the well-developed u from u_0^{qpc37} , the persistent shock-antishock structure (as already in u_0^{qpc37}). The shock contributes a $E(|k|)$ -component $\propto k^{-2}$ as already explicitly given in the zero-Hamiltonian u_0^{qpcK} in Eq. (16). So, the persistent structure and spectral tilt can not be simply related to ‘Hamiltonian effects’. With the parameterization of the model (15) as for the case in Fig. 3, the shock-antishock structure is still persistent but drifting slightly (not shown).

For the quantum revival and fractalization [16] (persisting into the nonlinear regime [17]) of the large- O model (15) with the QPC data, it remains to distinguish the mathematical limit and numerical limitation: how strong a nonlinearity the quantization effect can persist into is generally not clear so far [18].

Zero- λ solutions to the solitary-wave equation (4) are considered for insights associated to the Kolmogorov-Arnold-Moser (KAM) theorem: it is conjectured that a stationary $u_{s37}^{\#}$, responsible in the KAM fashion for the $u(x, t)$ developed from u_0^{qpc37} in Fig. 4, should be nearby, just as the comparison between u_0^{qpc5} and the stationary

$$u_{s5}^{\#} = 2(1 + \sqrt{3}) \cos x + 2 \cos(3x) + 2 \cos(5x), \quad (17)$$

calculated through the ansatz similar to Eq. (16) with $K = 5$. However, stationary $u_{sK}^{\#}$ s can be many for large K , and it is not clear how to identify the right one (if indeed); similarly for other Gr-systems.

Finally, as expected and observed in numerical experiments (not shown), QPC data with various Hamiltonian strengths add more longon states in the transient stages to the ‘particle

zoo’.

* jz@sccfis.org

- [1] P. J. Olver and P. Rosenau, Phys. Rev. E 53, 1900 (1996).
- [2] P. Rosenau, Phys. Rev. Lett. 73, 1737 (1994).
- [3] R. Camassa, D. D. Holm, and J. M. Hyman, Advances in Applied Mechanics 31, 1 (1994); R. Camassa and D. D. Holm, Phys. Rev. Lett. 71, 1661 (1993).
- [4] P. Rosenau and J. M. Hyman, Phys. Rev. Lett. 70, 564 (1993).
- [5] E. Tadmor, SIAM J. Numer. Anal. 26, 30 (1989).
- [6] C. S. Gardner, J. Math. Phys. 12, 1548 (1971).
- [7] R. Abramov, A. J. Majda, Methods and Applications of Analysis 10, 151 (2003); and references therein.
- [8] More extensive numerical results as well as other analyses such as the large- K limit will be for another communication: J.-Z. Zhu, preprint (2024).
- [9] S. C. Anco and M. L. Gandarias, arXiv:2401.00938 [math-ph]; P. Rosenau, J.M. Hyman, and M. Staley, Phys. Rev. Lett. 98, 024101 (2007).
- [10] This echoes the image of “Long” (in Chinese Pinyin for the oriental dragon), the force carrier for various interactions between, say, human and nature, which embodies the transformation between finitude and infinity, upholding order amidst potential chaos, and so on and so forth.
- [11] C. Bardos and E. Tadmor, Numer. Math. 129, 749 (2015).
- [12] Viewing all oscillations, even those traditionally deemed thermalized [7], as interacting solitonic longons may seem radical, yet it retains coherence.
- [13] U. Frisch, S. Kurien, R. Pandit, W. Pauls, S. S. Ray, A. Wirth, and J.-Z. Zhu, Phys. Rev. Lett. 101, 144501 (2008).
- [14] The large- O stiffness is overcome by the “ETDRK4” scheme of S. M. Cox and P. C. Matthews [J. Comput. Phys. 176, 430 (2002)].
- [15] For nonintegrable soliton turbulence, see, e.g., A. I. D’yachenko, V. E. Zakharov, A. N. Pushkarev, V. F. Shvets, and V. V. Yan’kov, Sov. Phys. JETP 69, 1144 (1989).
- [16] M. V. Berry, I. Marzoli, and W. Schleich, Physics World 14, 39 (2001); P. J. Olver, Am. Math. Monthly 117, 599 (2010).

- [17] G. Chen and P. J. Olver, *Discrete Contin. Dyn. Syst.* 34, 991 (2014).
- [18] G. Farmakis, J. Kang, P. J. Olver, C. Qu, and Z. Yin, arXiv:2309.14890 [math.AP].